Spectrally-selective coatings of gold nanorods on architectural glass

Nicholas L. Stokes, Jonathan Edgar, Andrew M. McDonagh, Michael B. Cortie*

*Institute for Nanoscale Technology, University of Technology Sydney, PO Box 123, Broadway NSW 2007, Australia; *author for correspondence (E-mail:michael.cortie@uts.edu.au)*

Key words : gold nanorods, solar spectrum, glazing, infrared absorption, coatings

Abstract

Infrared-blocking coatings on window glass can be produced by dispersing gold nanorods into a polymer coating. The spectral-selectivity of the coating is controlled by the shape and aspect ratio of the nanoparticles, which are in turn determined by the conditions applied during their synthesis. Coatings of nanorods in polyvinyl alcohol were deposited onto glass and characterized in both laboratory and sun-lit conditions. Selective attenuation of the near-infrared was demonstrated with the test panels transmitting approximately one third of the incident solar radiation, and absorbing nearly two thirds. The high absorptive cross-sections of the gold nanorods suggests that they can be applied in efficacious coatings at relatively low volume fractions.

Introduction

Glass windows in buildings are the site for significant heat transfer. A problem in cooler climates is outwards flow of heat during winter while inwards transfer of heat in summer is a significant issue in many tropical and temperate locations. The heat transfer occurs by a combination of conduction, convection and radiant mechanisms. Here we focus on the possible role of gold nanorods in controlling the passage of *radiant* solar energy through glass. Heat transfer due to

differences in air temperature is a separate issue and can be readily addressed by other technologies, such as double glazing.

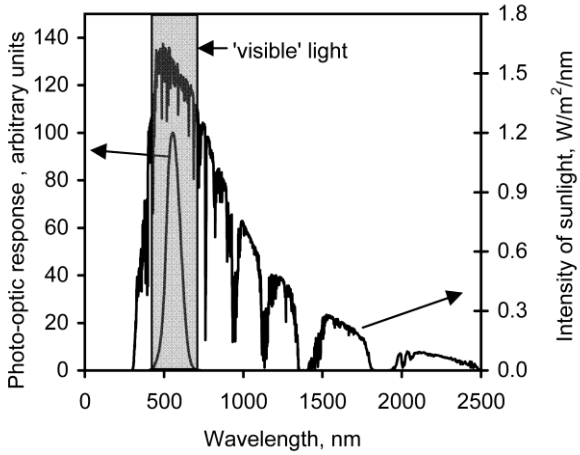

*Figure 1***.** The solar energy spectrum at the Earth's surface (hemispherical spectral solar irradiance for a sun-facing surface tilted at 37º, from ASTM G173 (G173-03, 2003)). The shaded section indicates the visible region. The photo-optic response of the human eye is also shown.

The sun can radiate up to 1000 W/m^2 in some parts of the world and the heat load on buildings from this source can be significant. The solar spectrum at the Earth's surface is reproduced in Figure 1 along with the photo-optic response of the human eye. In warm climates it is desirable that windows transmit as much visible light (400 to 700 nm) and block as much infrared radiation as possible. Given the nature of the solar spectrum on Earth, it is particularly desirable to attenuate the near-infrared region between 750 and 1300 nm as this contains an appreciable fraction of the invisible solar energy.

Transmittance through high quality 4 mm thick glass (Karisson et al., 2001) is about 90% over the spectral range 300 to 2500 nm but an acceptable level of optical transparency for architectural purposes would be maintained if up to 50% of the incoming visible spectrum was attenuated (Johnson, 1991). To achieve this, coatings may be designed to enhance the amount of radiation *reflected* from the surface of the window or alternatively to *absorb* radiation. A variety

of materials have been used or proposed for both classes of coating (Bell and Matthews, 1998, Granqvist, 2003, Schelm and Smith, 2003). Thin, reflective metal films, often of silver or gold, have been made using several different vacuum deposition techniques such as sputtering or ion plating, but these technologies are expensive relative to the relatively cheap absorbing materials available. In addition, legislation has been introduced in some cities that limit the amount of light that can be reflected by a building's facade. For example, in Sydney, Australia, the city council has limited the reflection of visible light from buildings to ~20% of that incident (Anon., 2008). The motivation is to prevent neighboring buildings being subjected to an increased glare.

The currently available absorptive coating schemes are based on either a dye (e.g. perylene or quaterrylene-based molecules) or a dispersion of infra-red absorbing semiconductors (Schelm and Smith, 2003, Granqvist, 2003). Of course, these coatings will conduct and convect approximately half of the absorbed heat inwards (Chowdhury et al., 2005) and therefore will be less efficient than reflective coatings but, because of the considerations mentioned above, interest in producing more efficient absorptive window coatings has increased significantly.

The ease of synthesis of gold nanoparticles of various shapes, the tunability of their plasmon resonances, and their excellent chemical stability have led various investigators to pursue their use in absorptive window coatings (Chowdhury et al., 2005, Xu et al., 2005, Xu et al., 2004, Pardiñas-Blanco et al., 2008, Shankar et al., 2005). The comparative merits of gold nanorods and nanoshells for spectrally-selective applications have been analyzed (Harris et al., 2008, Jain et al., 2006) and, although nanoshells have been previously considered for solar applications (Cole and Halas, 2006), we suggest that nanorods have the better optical characteristics and are easier to produce in large quantities and with controlled aspect ratios. The strongest plasmon resonance in gold nanorods occurs when the conduction electrons within the gold oscillate along the

longitudinal axis at the same frequency as the incoming light. The resonant frequency depends on the shape and aspect ratio (the ratio of length to width) of the nanorod (Murphy et al., 2005a, Xu and Cortie, 2006, Perez-Juste et al., 2005), with increasing aspect ratio associated with red-shifting of the resonance.

We have previously investigated the spectral-selectivity of coatings of nanometre-sized gold *hemispheres* on glass and found that they screen 17 to 28% of incoming infrared radiation, depending on their optical density (Chowdhury et al., 2005, Xu et al., 2005, Xu et al., 2004). In contrast, modeling showed that a window coating consisting of a mixture of gold nanorods with aspect ratios ranging from 3 to 10 would be much better than hemispheres and would effectively block light in the 800 to 1500 nm region (Xu et al., 2006). Although various schemes have been reported for directly attaching gold nanorods to glass (Niidome et al., 2004, Gole and Murphy, 2005, Gole et al., 2004, Wei and Zamborini, 2004, Xu et al., 2006), the resulting coatings were of insufficient optical density for our purposes. In contrast, it has been reported (Pérez-Juste et al., 2005, van der Zande et al., 1999) that gold nanorods could be readily dispersed in aqueous poly vinyl alcohol (PVA) from which thin polymer films of reasonable optical density could be obtained. The straightforward preparation and high optical density of the Au/PVA films led us to consider them here as a model for Au/polymer window coatings.

Experimental

Materials

The following chemicals were purchased commercially and used as received; hexadecyltrimethylammonium bromide (Nanjing Robiot), sodium salicylate (Ajax Finechem), ascorbic acid (Sigma Aldrich), silver nitrate (Sigma Aldrich) and potassium borohydride

(Sigma Aldrich), polyvinyl alcohol (Ajax Chemicals). Tetrachloroauric acid ($HAuCl_4$) was synthesized according to published methods (Breitinger and Herrmann, 1999). Water was purified by a MilliQ system. Glass (4 mm thickness) was manufactured by Viridian and purchased from R & R glass services, Australia. Glass panes were cut with dimensions 70 mm x 70 mm. The nanorod aspect ratios were measured using a Zeiss Supra 55VP scanning electron microscope.

Preparation of coatings on glass

Gold nanorods were prepared using a variation of the method of Murphy and co-workers (Jana et al., 2001, Murphy et al., 2005b). Briefly, for aqueous nanorod solutions consisting of nanorods of 3.4 aspect ratio, we used 10.93 g hexadecyltrimethyl ammonium bromide (CTAB) diluted in 150 mL water, 1.5 mL 0.1 M tetrachloroauric acid ($HAuCl_4$), 1.5 mL 0.1 M sodium salicylate, 1.65 mL 0.1 M ascorbic acid, and 2.25 mL 0.01 M silver nitrate ($AgNO_3$), diluted to 300 mL. Nanorods of 3.9 aspect ratio were prepared using 14.58 g CTAB dissolved in 200 mL water, 2 mL 0.1 M $HAuCl_4$, 2 mL 0.1 M sodium salicylate, 2.2 mL 0.1 M ascorbic acid, and 4 mL of 0.01 M $AgNO_3$. This solution was then diluted to 400 mL. Growth was initiated by addition of 1% v/v of seed solution to the growth solution. The seed solution was prepared by adding 0.5 mL of ice-cold potassium borohydride (0.01 M) to 10 mL of a solution containing $HAuCl_4$ (0.125 mM) and CTAB (25 mM). The resultant suspensions were centrifuged and washed with water. The two rod samples are designated as ‘R1’ and ‘R2’ hereafter. The aspect ratio of the rods is controlled by the amount of $AgNO_3$ added but larger additions than those used here brought no advantage because they decreased the yield of nanorods.

R1 and R2 were mixed into 15 wt% PVA solutions in various ratios and then cast into a 2 mm deep recess on glass panes and allowed to dry to form thin films. The final thickness of the film was ~0.8 mm. The optical densities of these thin films were controlled by the concentration of the initial gold nanorod solutions.

Characterization of coatings

Reflection and transmission spectra were collected between 300 and 2500 nm using a Perkin Elmer Lambda 950 UV/VIS/NIR spectrophotometer. This data were then convoluted with the standard ASTM AM1.5 solar spectrum (G173-03, 2003) to give an estimate of the solar screening efficacy of the coated glass panes. The optical properties of these larger area samples were also tested outdoors in natural sunlight using a thermopile to measure the incident and transmitted intensity. We considered this to give a more realistic simulation of the coating's overall performance than use of lamps in an indoor laboratory setting. A thermocouple was used to measure the temperature of the glass, film and ambient air. The panes were oriented so that they were normal to the direction of sunlight and measurements were made between 09:00 and 12:00 on two clear days in Sydney, Australia. The solar irradiance was 870 ± 5 W/m^2 at 10:30 am and increased to 885 ± 5 W/m^2 at 12:00 pm. Wind speed was measured using a Digitech anemometer. Average wind speed during measurements was between 0 – 3 km/hr with occasional gusts of up to 7 km/hr.

The thermopile detector, (PMA 2143, from Solar Light Company, USA) provided a linear response to radiation between 200 and 50000 nm and had an angular field-of-view of 9°. Recording the transmission of the film required the thermopile to be set behind the window and the intensity was recorded at 90° to the plane of the glass. Direct reflection, on the other hand,

could not be measured due to the shadow cast onto the glass by the thermopile. Instead, reflection data was obtained from the laboratory spectra. The remaining solar radiation must have been either absorbed by the samples, or re-radiated at high angles (>9º) off the front and back surfaces. Any absorbed radiation will cause the glass to heat up and the energy will thereafter be both convected and re-radiated to the surrounding environment. However, thermal re-radiation at these low temperatures can be neglected and the dominating form of heat transfer off the glass will be convection.

Heat convection of the front and rear surfaces of the glass panes was estimated from

$$q_{convected} = (T_S - T_{Air})A\bar{h} \qquad (1)$$

where T_s is the temperature of the window surface, A is the area of the glass and $\bar{h}$ is the average heat transfer coefficient over the pane. The latter can be estimated from

$$\bar{h} = \frac{Nu_L.k}{L} \qquad (2)$$

where Nu_L is the average Nusselt number over the glass pane, *k* is the thermal conductivity of air and *L* is the height of the glass pane. There are many empirical correlations for Nu_L. In our case we used a generic expression (Holman, 1990) for forced convection over an evenly heated plate:

$$Nu_L = 0.228\,\mathrm{Re}_L^{0.731}\,\mathrm{Pr}^{1/3} \qquad (3)$$

The condition of 'forced' (rather than 'natural') convection was used because the experiment was conducted outdoors with an inevitable light breeze. The Prandtl number (*Pr*, which relates the relative thicknesses of the hydrodynamic and thermal boundary layers) is approximately 0.71

for air at temperatures between 0 and 50ºC, and the average Reynolds number (Re_L, which is related to the transition from lamellar to turbulent flow) over the pane is given by

$$Re_L = \frac{u_\infty L}{\nu} \tag{4}$$

where u_∞ is the fluid velocity. The kinematic viscosity, ν is approximated by

$$\nu = \frac{\mu}{\rho} \tag{5}$$

where ρ is the density of air, and μ is the dynamic viscosity and may be obtained from tables. It is about 15×10^6 m^2/s at 27ºC (Holman, 1990).

Finally, measured temperatures from the window and surroundings were used in conjunction with the above equations to estimate the heat convected and radiated from the front and rear of the glass panes.

Simulation of optical performance

The optical properties of gold nanoparticles can be accurately predicted by calculations made using the discrete dipole approximation provided that the dipole spacing is sufficiently small (Myroshnychenko et al., 2008). Here we used the DDSCAT code of Draine and Flatau (Draine and Flatau, 1994, Draine and Flatau, 2008) to simulate the optical extinction efficiency of the nanoparticles. A dipole spacing of about 1 nm was used. Because the experimental rods had a range of aspect ratios, the transmission spectra of the rods were simulated by calculating a weighted average extinction cross-section over a range of simulated rod shapes, with the shapes chosen drawn from the distribution of shapes represented in the experimental sample. The solution absorbance, A, is related to the extinction cross-section of a nanoparticle by:

$$A = \log_{10} \frac{I_0}{I(x)} = \frac{N.C_{ext}.x}{2.303} \quad (6)$$

where N the number of particles per unit volume, C_{ext} the extinction cross-section, x the optical path length, I_0 the incident flux and $I(x)$ the transmitted flux (Perez-Juste et al., 2005).

From this, the transmittance of the coatings, $I(x)/I_0$, is:

$$\frac{I(x)}{I_0} = 10^{-A} \quad (7)$$

Solar Heat Gain Coefficient (SHGC)

The total incident energy can be found from equation

$$q_{incident} = q_{reflected} + q_{transmitted} + q_{convected(f)} + q_{convected(b)} + q_{radiated(f)} + q_{radiated(b)} \quad (8)$$

where *f* and *b* refer to front and back faces respectively. The radiant energy passing through the window is $q_{transmitted} + q_{radiated(b)}$ and the radiant energy shed from the front window face is $q_{reflected} + q_{radiated(f)}$. $q_{incident}$ is a well characterized value as it can be measured or estimated from standard tables. $q_{transmitted}$ and the majority of $q_{radiated(b)}$ can be obtained by measurement (note that the detector used had a field-of-view of 9º, therefore any $q_{radiated(b)}$ at greater angles than this was ignored, and summed instead into the absorbed, ie. convective, component of the energy balance). Finally, $q_{convected}$, both front and back were estimated from the surface temperature of the glass and the principles of convective heat transfer. Equation 9 shows the proportion of energy that is transferred to the interior environment. As $q_{incident}$ is solar radiation, $F = F_{solar}$ is the solar heat gain coefficient (SHGC) (Dai, 2001).

$$F = \frac{q_{transmitted} + q_{convected(b)} + q_{radiated(b)}}{q_{incident}} \quad (9)$$

The SHGC of the coated glass panes was determined by two means. First, the transmission and reflection spectra of the samples were convoluted with a standardized solar spectrum and the expected energy balance over the sample calculated. Second, samples were exposed to natural sunlight outdoors and the energy balance over the sample was estimated by calculation of the expected convective and radiative transfer of heat, taken in conjunction with the actual solar irradiance. Naturally, the two approaches would be expected to produce a similar estimate of SHGC.

Results and Discussion

Optical properties of gold nanorods and films

The shape of the nanorods approximated a hemispherically-capped right-cylinder. A representative sample is shown in Figure 2(a). The distribution of aspect ratios was determined for the suspension with an extinction peak at 770 nm, R1, by inspection of SEM micrographs of dried portions of the suspension. From the data shown in Figure 2(b), the mean length and diameter of this sample of rods was 47.1 (s=5.5) nm and 12.7 (s=1.6) nm, n=94 (standard deviation in parentheses).

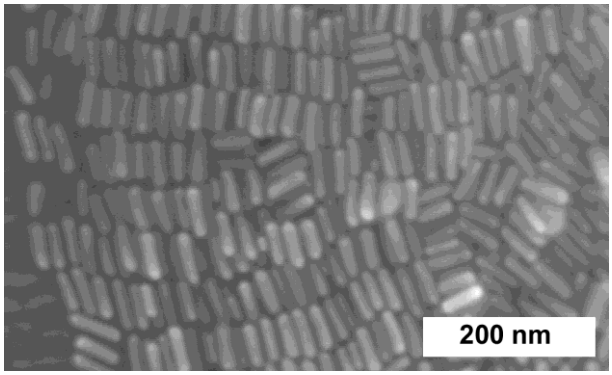

(a)

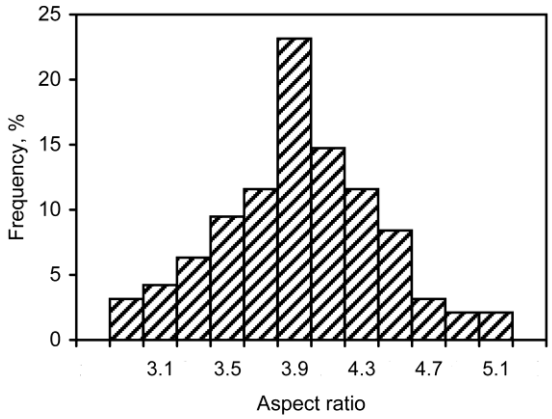

(b)

Figure 2. (a) Scanning electron micrograph of gold nanorods sample R1 used in the present work. (b) Distribution of aspect ratios in sample R1.

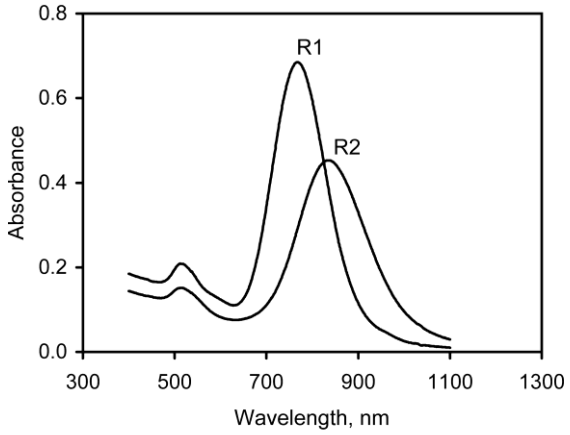

Figure 3. Optical absorbance spectra of two suspensions of gold nanorods, R1 (absorption maximum at 768 nm) and R2 (absorption maximum at 834 nm).

The optical transmission spectra of 'R1' and 'R2' in solution are shown in Figure 3. The lower wavelength of maximum extinction for R1 indicates that these rods have, on average, shorter aspect ratios than R2. Comparison of the experimental optical data with calculated extinction spectra for rods of different aspect ratios revealed that the measured extinction bands are much broader than would have been the case for a monodisperse sample of rods. To investigate this further, the measured spectrum was simulated by combining the weighted average of twenty five calculated spectra of rods with a distribution of shapes matching the experimental distribution discussed above. Figure 4 shows the simulated spectrum together with the experimental spectrum. The calculated extinction (dashed line) is in close agreement with the measured extinction spectrum. Therefore, the transmission spectrum of R1 shown in Figure 3 represents the ensemble average produced by a range of rod sizes with a distribution similar to that shown in Figure 2(b). We also found that extinction peaks at any intermediate wavelength could be obtained by mixing R1 and R2 in an appropriate ratio. Blending of R1 and R2 also has the effect

of broadening the extinction peak, which may be desirable in solar screening applications (Xu et al., 2006). The ratios chosen for the production of PVA coatings on large glass panes were (1) 50:50 R1 and R2, and (2) 33:67 R1 and R2. These two samples are designated as 'Pane 1' and 'Pane 2' respectively. The former mixture maximized the width of the near-IR extinction trough while the latter sample allowed us to probe the effect of shifting the absorption peak further into the infrared. The samples were examined in a scanning electron microscope, Figure 5. The PVA coating has a distribution of well-separated gold rods and the coating thickness of 800 μm provides a high likelihood that incident photons will encounter the gold nanoparticles.

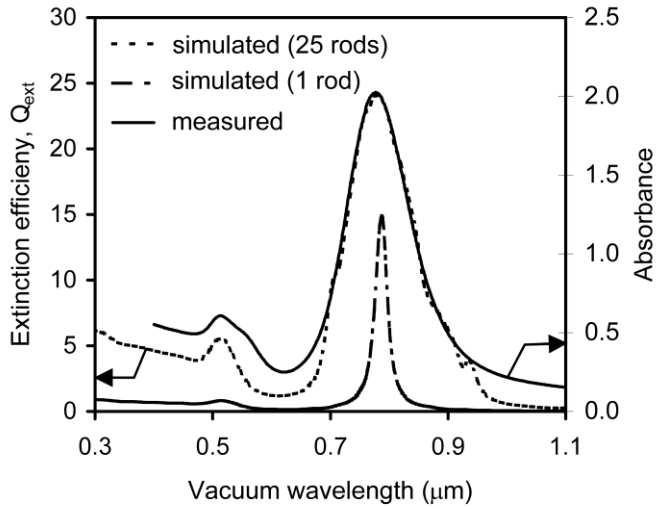

Figure 4. Comparison of the measured extinction properties of the nanorods with an extinction spectrum obtained by direct numerical calculation of the optical properties of an ensemble containing twenty five different shapes of rod drawn from the distribution shown in Figure 2(b). Also shown for purposes of comparison is the simulated DDA extinction spectrum for a single rod with an aspect ratio of 3.9.

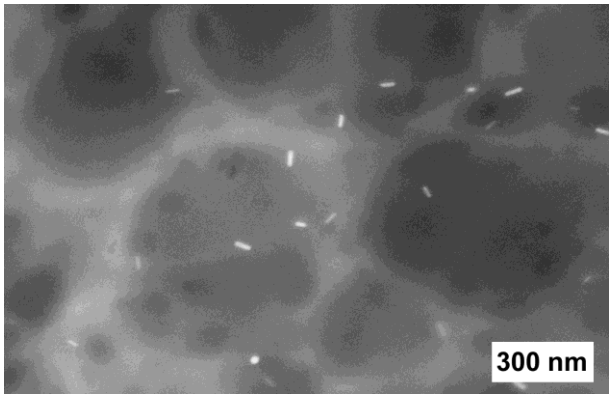

Figure 5. Scanning electron microscope image of the surface of the Au nanorod/PVA coating. the electron beam penetrates some tens of nanometers into the PVA and individual rods can be discerned. The cellular structure of the PVA is an artifact produced by damage induced by the electron beam.

Transmission and specular reflectance data are shown in Figure 6. Samples of plain glass and plain glass coated with PVA only are hereafter designated 'Glass' and 'Glass-PVA', respectively. Glass exhibits a broad band in its NIR transmittance with a minimum at 1058 nm. Relatively low reflection values (<12 %) were recorded for all of the measured samples including Pane 1 and Pane 2. This indicates that gold nanorod coatings in PVA are suitable in locations where highly reflective coatings are unsuitable. The absorption peaks between 1400 and 2500 nm for the samples Glass-PVA, Pane 1 and Pane 2 are due to the PVA, and the absorption peaks from 400 through to 1400 nm in Pane 1 and Pane 2 are primarily due to the gold nanorods. The large transmission minimum at ~810 nm coincides with the expected position of the longitudinal resonance of rods dispersed in PVA. PVA has a refractive index of 1.52, which is higher than that of water and results in a red-shift of the longitudinal plasmon resonance compared to that of rods in aqueous solution (see Figure 4.) The average transmission in the visible is approximately 35% for both samples. At 800 nm, Pane 1 and Pane 2 have reflection and transmission values of ~5%, implying that at this wavelength the absorbance

accounts for ~90% of the incoming light. Pane 2, however, absorbs more light in the range 900 - 1400 nm and is thus more suited for use as an absorptive window coating than Pane 1.

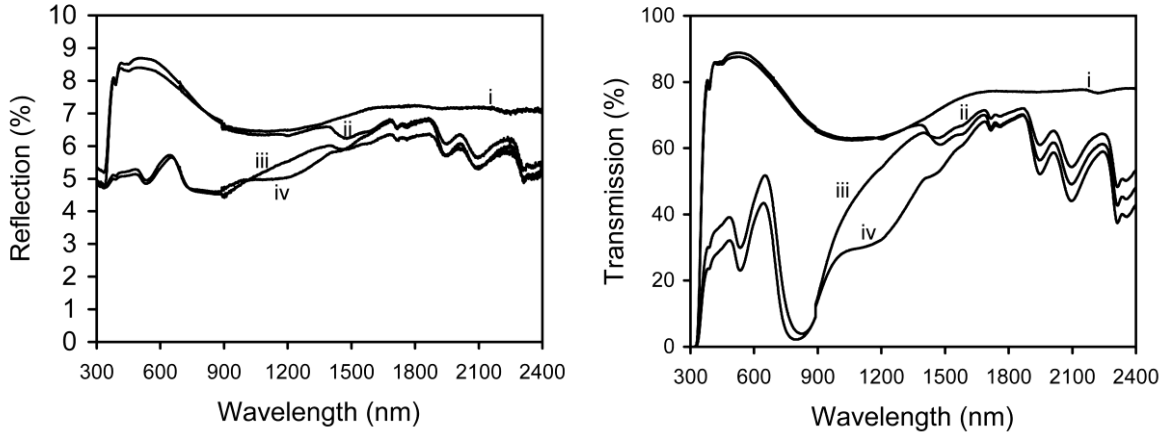

(a) (b)

Figure 6. (a) Reflection and (b) transmission spectra of (i) 4mm clear glass, (ii) PVA-glass, (iii) Pane 1 and (iv) Pane 2.

Calculation of the SHGC from the optical spectra

Calculated thermal properties are shown in Table 1. The very small amount of thermal re-radiation that would occur from the back face is neglected. The optical transmission spectrum of Pane 1 indicates that it should have passed only 329 W/m^2 by transmission when illuminated with sunlight at 885 W/m^2, and that 46 W/m^2 should have been reflected. Therefore, the difference, 530 W/m^2, would have been absorbed and shed by convective heat transfer. If the velocity of air on both sides of the pane was identical then, because the temperature gradient across the glass is small, approximately equal amounts of this thermal energy would be shed on the 'inner' and 'outer' surfaces of the window by convection, allowing for an estimate of F_{solar},

designated here as $F_{sol\text{-}1}$ to differentiate it from $F_{sol\text{-}2}$, the estimate obtained under outdoors conditions (see next section).

Table 1. Calculated optical properties for plain glass, plain glass coated with PVA, and the glass panes coated with Au nanorods, with reference to the ASTM G173 standard solar spectrum.

Sample	Transmitted %	Reflected %	Absorbed % (by difference)	$F_{sol\text{-}1}$ % (for equal airspeeds on both sides of pane)
Glass	75.3	7.4	17.3	84.0
Glass-PVA	74.0	7.4	18.7	83.4
Pane 1	37.2	5.2	57.6	66.0
Pane 2	29.2	5.2	65.6	62.0

Estimation of the SHGC under 'natural' conditions

The accuracy of the measurement under natural conditions is strongly influenced by whichever empirical correlation is used for the Nusselt number, which in turn is also influenced by the wind speed at the time of measurement. The transmission through the sheet of commercial quality glass used as a reference sample was ~691 W/m^2 on the day, which is ~77 % of the 897 W/m^2 of solar radiation being received at that time. Therefore 23 % of the solar irradiance on this sample must have been absorbed or reflected. The temperature of the clear glass was measured to be 21.2°C and the outside temperature was 15.0°C, giving an increase of 6.2°C. Using the measured temperature, the heat convected off each face of the clear glass is calculated to be between 52 W/m^2 and 87 W/m^2 for wind speeds of between 0.5 and 1 km/hr respectively. Since there are two sides to the glass, it is evident that between 11 and 19% of the incoming radiation was absorbed

and shed as heat. This fits with the figure obtained above by consideration of the measured optical property data for clear glass and the standard solar spectrum. Table 2 shows the performance of coated Panes 1 and 2 compared to the clear glass sample using the same methodology.

Table 2. Performance of Au/PVA samples compared to clear glass. Samples were measured outside under normally incident illumination from the sun. The wind speed ranges are given in parentheses.

	Incident flux	ΔT, °C		T	Convected energy		R	F_{sol-2}
	W/m^2				%	%	%	%
		front	back	%	front	back		
Glass	897±5	6.2	6.2	77.1	5.8 - 9.7 (0.5-1.0 km/h)	5.8 - 9.7 (0.5-1.0 km/h)	7.4	82.9 - 86.8
PVA-Glass	909±5	6.3	6.1	75.0	5.9 - 9.7 (0.5 - 1 .0 km/h)	5.7 - 9.4 (0.5 - 1.0 km/h)	7.4	80.7 - 84.4
Pane 1	885±5	9.5	6.2	34.9	35 - 47 (2-3 km/h)	22.8 – 30.7 (2-3 km/h)	5.2	57.7 - 65.6
Pane 2	885±5	10.9	8.2	31.2	40.1 - 54 (2-3 km/h)	30 – 40.6 (2-3 km/h)	5.2	61.2 - 71.8

Panes 1 and 2 have 40% and 37%, respectively, of the incoming energy being either transmitted and reflected, leaving 60% and 63% to be absorbed and then convected. Of this, the slightly larger proportion was convected from the surface facing the sun due to it having a higher temperature. Therefore, somewhat less will be convected from the rear surface. In fact, since indoor air velocity is generally much lower than outside, the F_{solar} values of such coatings would in general be even better than those shown here.

Whereas the SHGC for a coating provides a direct indication of the attenuation of solar radiation, it does not fully describe the efficacy of a coating system. An additional method to compare the efficiency is the T_{lum}/T_{sol} ratio, which is a measure of the overall ability of the

window to selectively transmit light visible to the eye whilst blocking infrared radiation (Dai, 2001, Smith et al., 1986, Chowdhury et al., 2005). T_{lum}, the transmitted visible proportion of the spectrum weighted by the photo-optic response of the human eye, can be found from

$$T_{lum} = \frac{\int_{380}^{760} T_\lambda V_\lambda \cdot E_\lambda \cdot d\lambda}{\int_{380}^{760} V_\lambda \cdot E_\lambda \cdot d\lambda} \qquad (10)$$

where λ is the wavelength, T_λ is the total spectral transmissivity of glass as a function of λ, V_λ is the photo-optic luminous efficiency function of the human eye as a function of λ and E_λ is the spectral irradiance of the light source as a function of λ. The limits of the integration are the wavelength in nm. T_{sol}, the proportion of the solar irradiance transmitted can be found from

$$T_{sol} = \frac{\int_0^\infty T_\lambda E_\lambda \cdot d\lambda}{\int_0^\infty E_\lambda \cdot d\lambda} \qquad (11)$$

The maximum possible ratio of T_{lum}/T_{sol} is 2.08 for a window coating that allows through all visible wavelengths and blocks all invisible wavelengths, ie. provides a maximum T_{lum} and a minimum T_{sol}. More realistic representative values include 0.99 for a dye based coating, 1.04 for a metallized coating and 1.7 for a state-of-the-art optimum spectrally selective coating (Dai, 2001). The parameters obtained for the present samples are summarized in Table 3. Also shown are the CIE *L*a* b** color parameters for the glass, as perceived in transmission using ASTM D65 white light as the illuminant. The figure-of-merit for both panes was about unity, indicating that they do not selectively attenuate the thermal part of the spectrum relative to the visible. This is a situation that is comparable to the commercial products available at the cheaper end of the solar glazing market.

Table 3. Figures-of-merit determined for present samples. $T_{sol\text{-}1}$ is calculated from the measured transmission spectrum. $T_{sol\text{-}2}$ was measured under outdoors conditions and is equivalent to the 'transmittance' in Table 2.

Sample	T_{lum}	$T_{sol\text{-}1}$	$T_{sol\text{-}2}$	$T_{lum}/T_{sol\text{-}1}$	CIE L^*	CIE a^*	CIE b^*	Color
glass	0.87	0.76	0.78	1.15	94.6	-1.7	0.6	blue tinge
PVA on glass	0.87	0.74	-	1.19	95.1	-1.8	0.9	blue tinge
Pane 1	0.37	0.37	0.35	1.00	67.1	11.1	-0.3	purple
Pane 2	0.30	0.29	0.31	1.03	61.7	12.4	0.3	purple

The slight purple tinge of the panes is the result of the cylindrical rods used having a minimum in absorbance between 600 to 650 nm. This absorption minimum can be eliminated if desired by the use of 'dog-bone' shaped nanorods, which have an additional transverse plasmon resonance over this range of wavelengths (Xu and Cortie, 2006). A typical spectrum of dog-bone shaped rods produced by increasing the sodium salicylate concentration is shown in Figure 7. A coating made with such rods would display a color ranging from dark blue to grey blue (CIE L=58.4, a^*=-4.9, b^*=-9.2) , depending on the concentration of dog-bones.

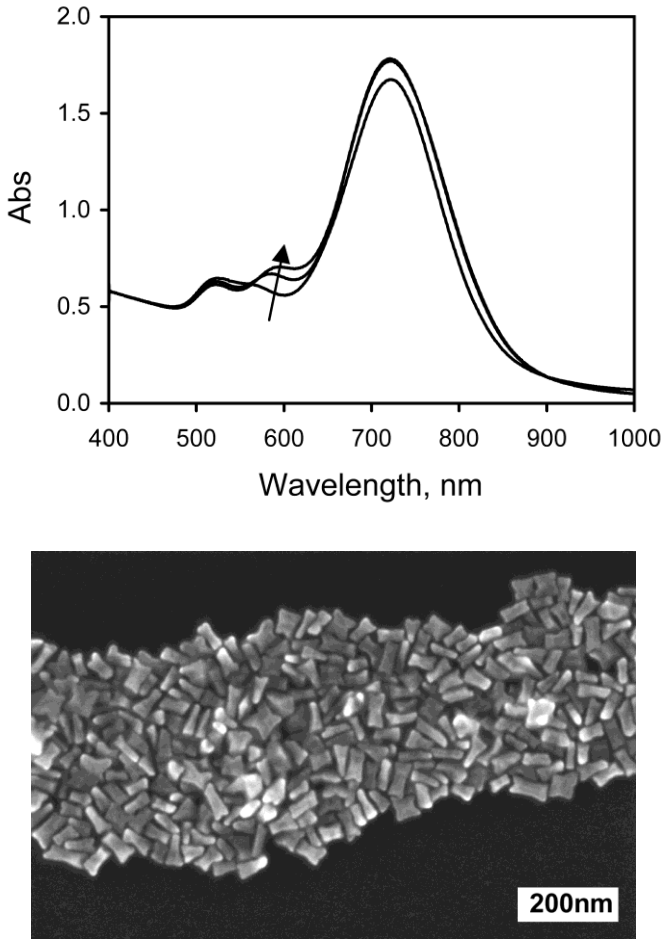

Figure 7. (a) Extinction spectrum of a suspension of gold 'dog-bones' The development of a 'dog-bone' shape in the nanorods can be used to nullify the pink tinge produced by the transverse plasmon resonance. The samples shown here were obtained by increasing the sodium salicylate concentration from 0 to 2 mM, in the direction of the arrow. (b) Example of Au dog-bones, in this case produced with a sodium salicylate concentration of 1.0 mM.

Conclusions

Gold nanorods have a well-defined optical extinction peak, the position of which is readily tuned by adjustment of the aspect ratio. Nanorods of different aspect ratios can be blended to produce a spectrally selective coating suitable for solar glazing applications. The samples discussed here transmitted between 30 and 37% of the luminance of sunlight while having a Solar Heat Gain Coefficient of between 58 and 72% relative to the total incoming heat flux. The difference between these two values is characteristic of absorptive coatings, which must necessarily shed heat by convection. Up to half of this heat load must be transferred off the inner face of the coated glass which decreases the thermal efficacy of absorptive systems. This may be offset in some applications by the fact that these systems do not reflect heat load onto adjacent buildings, and may be cheaper to produce. The incorporation of gold nanorods of even greater aspect ratios than used here, or with dog-bone morphologies, would increase their effectiveness as a window coating even further. The color of the transmitted light can be varied from purple to grey-blue by control of the nanoparticle shape.

Acknowledgements

This work was supported by AngloGold Ashanti Limited, AGR Matthey and the Australian Research Council. We thank Mr Martin Blaber for assistance with the calculations.

References

Anon. (2008) Standard Conditions of Development Consent in Planning. Sydney City Council, Australia.

Bell JM, Matthews JP (1998) Glazing materials Materials Forum 22:1-24.

Breitinger D, Herrmann W (1999) Synthetic Methods of Organometallic and Inorganic Chemistry, Stuttgart, George Thieme Verlag.

Chowdhury H, Xu X, Huynh P, Cortie M (2005) Radiative Heat Transfer Across Glass Coated With Gold Nano-Particles J Sol Energ-T ASME 127:70 - 75.
Cole JR, Halas NJ (2006) Optimized plasmonic nanoparticle distributions for solar spectrum harvesting Appl. Phys. Lett. 89:153120.
Dai Y (2001) Solar control film retrofitted energy efficient windows for tropical climate. Proc. Glass Processing Days 2001. Tampere, Finland, Tamglass Ltd Oy.
Draine BT, Flatau PJ (1994) Discrete-dipole approximation for scattering calculations J. Opt. Soc. Am. A 11:1491-1499.
Draine BT, Flatau PJ (2008) User Guide for the Discrete Dipole Approximation Code DDSCAT 7.0 http://arxiv.org/abs/0809.0337, accessed September 2008
G173-03 (2003) Standard Tables for Reference Solar Spectral Irradiances: Direct Normal and Hemispherical on 37° Tilted Surface. American Society for Testing and Materials (ASTM).
Gole A, Murphy CJ (2005) Polyelectrolyte-coated gold nanorods: synthesis, characterization and immobilization Chem. Mater. 17:1325-1330.
Gole A, Orendorff CJ, Murphy CJ (2004) Immobilization of gold nanorods onto acid-terminated self-assembled monolayers via electrostatic interactions Langmuir 20: 7117-7122.
Granqvist CG (2003) Solar energy materials Adv. Mater. 15:1789-1803.
Harris N, Ford MJ, Mulvaney P, Cortie MB (2008) Tunable infrared absorption by metal nanoparticles: the case for gold rods and shells Gold Bull. 41:5-14.
Holman JP (1990) Heat Transfer. Seventh Edition., London, McGraw-Hill.
Jain PK, Lee KS, El-Sayed IH, El-Sayed MA (2006) Calculated absorption and scattering properties of gold nanoparticles of different size, shape, and composition: applications in biological imaging and biomedicine J. Phys. Chem. B. 110:7238-7248.
Jana NR, Gearheart LA, Murphy CJ (2001) Wet chemical synthesis of high aspect ratio cylindrical gold nanorods J. Phys. Chem. B 105:4065-4067.
Johnson T (1991) Low-E Glazing Design Guide, Boston, Butterworth Architecture.
Karisson J, Karlssson B, Roos A (2001) Performance of antireflection glazings in windows. Proc. Glass Processing Days 2001. Tampere, Finland, Tamglass Ltd Oy.
Murphy CJ, Sau TK, Gole A, Orendorff CJ (2005a) Surfactant-directed synthesis and optical properties of one-dimensional plasmonic nanostructures MRS Bull. 30:349-355.
Murphy CJ, Sau TK, Gole AM, Orendorff CJ, Gao J, Gou L, Hunyadi SE, Li T (2005b) Anisotropic metal nanoparticles: synthesis, assembly, and optical applications J. Phys. Chem. B 109:13857-13870.
Myroshnychenko V, Rodríguez-Fernández J, Pastoriza-Santos I, Funston AM, Novo C, Mulvaney P, Liz-Marzán LM, de Abajo FJG (2008) Modelling the optical response of gold nanoparticles Chem. Soc. Rev. 37:1792 - 1805.
Niidome Y, Takahashi H, Urakawa S, Nishioka K, Yamada S (2004) Immobilization of Gold Nanorods on the Glass Substrate by the Electrostatic Interactions for Localized Plasmon Sensing Chemistry Letters 33:454-455.
Perez-Juste J, Pastoriza-Santos I, Liz-Marzan LM, Mulvaney P (2005) Gold nanorods: synthesis, characterization and applications Coordin. Chem. Rev. 249:1870-1901.
Pérez-Juste J, Rodríguez-González B, Mulvaney P, Liz-Marzán LM (2005) Optical control and patterning of gold-nanorod-poly(vinyl alcohol) nanocomposite films Adv. Funct. Mater. 15:1065 - 1071.
Schelm S, Smith GB (2003) Dilute LaB_6 nanoparticles in polymer as optimized clear solar control glazing Appl. Phys. Lett. 82:4346-4348.

van der Zande BMI, Pages L, Hikmet R, van Blaaderen A (1999) Optical Properties of Aligned Rod-Shaped Gold Particles Dispersed in Poly(vinyl alcohol) Films Journal of Physical Chemistry B 103:5761-5767.

Wei Z, Zamborini FP (2004) Directly monitoring the growth of gold nanoparticle seeds into gold nanorods Langmuir 20:11301-11304.

Xu X, Cortie MB (2006) Shape change and color gamut in gold nanorods, dumbbells and dog-bones Adv. Func. Mater. 16:2170-2176.

Xu X, Cortie MB, Stevens M (2005) Effect of glass pre-treatment on the nucleation of semi-transparent gold coatings Mater. Chem. Phys. 94:266-274.

Xu X, Gibbons T, Cortie MB (2006) Spectrally-selective gold nanorod coatings for window glass Gold Bull. 39:156-165.

Xu X, Stevens M, Cortie MB (2004) In situ precipitation of gold nanoparticles onto glass for potential architectural applications Chem. Mater. 16:2259-2266.